DESIGN OF A THREE-PHASE AXIAL FLUX SELF-EXCITED INDUCTION GENERATOR IN INDUSTRIALS DISCHARGE CHANNELS

Ricciotti, A. C. D.[1], Ricciotti, V. B. S. D.[2], Militão, H. S. G.[3], Andrade, G. P.[4], Braga Jr., Adailton[3]

[1,2]Professor, Dept. of Electrical Engineering, Federal University of Rondônia, Brazil
[3]Researcher, GPTI - Federal University of Rondônia, Brazil
[4]Eng. Process Optimization Coordinator, TERNIUM, Brazil

---***---

Abstract - *The feasibility of obtaining electric energy in water flows, regardless of size, imposes environmental modifications subject to authorization processes with government agencies, which demand time and with financial costs impacting on the investment. The present article presents a floating hydroelectric generation system using an A three-phase axial flux self-excited induction generator conjugated to a floating crossflow hydrokinetic converter, Michell-Banki type, for the generation of electrical energy from the use of water flows in rivers, environmentally possible and low impact*.

Key Words: Three-phase Self-Excited Induction Generator, Hydrokinetic Turbine, Axial Flux Self-Excited Induction Machine.

1. INTRODUCTION

The high-power hydroelectric generation focused on the construction of large power plants requires the full use of water courses, even with small differences in terrain, causing, in most cases, significant flooding of areas occupied with anthropogenic activities. The problems related to the eviction process involve high environmental, economic, and social costs, besides the various legal embargoes, common in these types of enterprises. The fact is that the different technologies of the electric machines used have a high cost of manufacturing and complicated installation.

The idea of using smaller generators and of lower environmental impact at various points in water flow can provide enough electricity to meet the same demand for large enterprises with the decreased ecological, economic and social costs, as well as the constructive simplicity of generators and its maintenance.

The energy utilization of low flow velocity watercourses, frequently, uses induction machines or generator radial flux permanent magnets given the low manufacturing cost. The hydrokinetic conversion systems used to involve different technologies, and the use of Michell-Banki (water wheel) type turbines is widespread where the electric machine is coupled employing rigid shafts, belts or chains.

Radial flux electrical machines are most significant than axial flux self-excited induction (AFSEI) and have several applications and advantages that include higher power/weight ratio, and their stator and disk rotor enable better adjustments in the air gap. The combination of AFSEI machines with Michell-Banki type hydrokinetic converter in only equipment combines, in addition to the smaller space, the ease of installation with the possibility of use in floating or submerged [1] - [6]. The present article aims to present the constructive aspects of a hydrokinetic generator that works on the surface of a water flow, whose structure allows to obtain performance even for low speeds.

1.1 Crossflow Hydrokinetic Converter

In hydrokinetic converters, the output power level is directly related to the flow velocity and the various technologies developed for small flows, mainly turbines in their different configurations. Michell-Banki type crossflow turbines use a drum-type rotor equipped with blades. In this case, water flows directed by a hydraulic profile and encounters the rotor blades, moving it, in the hydraulic operations with smaller falls and a higher volume of water use this type of turbine. The different types of couplings used between the turbine and the generator result in problems ranging from the difficulty of balancing the axes, exposing parts to the elements, increasing the space used, and even the maintenance. The construction of different equipment combining a hydraulic crossflow converter with a permanent magnet generator or squirrel cage induction motor in the axial flux machine allows space gain, support, and more power.

Some models in use that use generators on the same axis of the turbine rotor, like the bulb turbines, have flow parallel to this axis and of this form they need control in their speed. A generator model integrated to the rotor core of a turbine to compose a generator was proposed by [1], the water flow passes outside the turbine, as the wind generators. Another model based on wind turbine studies, introduced by [2], describes an axial hydrokinetic turbine, which works through the kinetic energy due to the passage of water, externally, by the rotor.

Many companies around the world have invested in the development of hydrokinetic technologies with different specifications, operating speeds, and maximum power delivered. In [3] and [4] show revisions about techniques employed by some companies in the world.

The company Smart Hydro Power [4] developed a hydraulic turbine project on the world stage. The German-based company has sold more than 40 turbines since 2010, the year the company was inaugurated with projects in countries like Peru, Colombia, Nigeria, India, and Indonesia. The turbine has a generator coupled to the rotor shaft. A diffuser in the back to optimize water flow, two floats to maintain stability, this turbine also features the version with a floating. The power generation can reach 5kW, the rotor is 1 meter in diameter and operates at speeds between 90 and 230 rpm, the turbine is 1.12 meters in height and the same value in width, 2.6 meters in length.

Rutten Company, Herstal, Belgium, has developed a floating tubular turbine concept using water wheels and is testing in Zaire, Africa. In the article "Small-scale-water-current-turbines-for-river-applications" [3], the author makes an extensive review of the work on hydrokinetic converters for low flow velocities, without a similar quote to the proposal. Other articles of this type do not mention the contributions of new technologies to these converters.

New works on technological innovation in the generation of electric energy through hydrokinetic plants are scarce and refer to known models and their adaptations. In Brazil, the Mechanical Engineering Department of the University of Brasilia was the first turbine project to be completed in 1987. Several turbine projects followed, but the first to be installed was called Generation 1 [1], in the municipality of Correntina, Bahia. Sometime later, a second turbine called the second generation developed. Some innovations made in this new equipment, a conical diffuser was coupled to the machine to decelerate the flow at the output of the turbine, creating a low-pressure region, increasing the inflow velocity and power factor of the engine. As a disadvantage, the new configuration showed that the dimensions were most significant than the first model and had restricted use in rivers with a depth of at least 2 meters. With the performance of the third turbine increased, in the version the rotor was coupled to the rest of the equipment, operating inside the water connected to the shaft. There was a new design for the diffuser, contributing to the best performance. For this turbine, the use of the new diffuser dramatically improves the efficiency of the machine.

A new concept of the vertical hydraulic turbine with rotor conjugated to the stator and axes positioned axially to that of the fluid flow [4] has been patented and works submerged or in line with pipes where there are flows of any kind [5].

1.2 Axial Flux Self-Excited Induction Generator

The first electric machines invented were those of axial flux, and since the Davenport patent in 1837, the radial flux machines have dominated the market. In the last decade's radial electric engines have been very successful in terms of electric generators. However, they are enormous and heavy. Due to the geometric considerations, an enticing alternative in the market is AFSEI machine, when the length of the engine and high torque are limiting and desired factor.

On the other hand, a new degree of freedom of an axial flux machine is the possibility of several relations between the stator position and the rotor positions, making it possible to select the most appropriate machine structure for the given application. Axial flux motors have two topologies [7]. The single-sided topology has as main characteristic a construction formed only by a rotor and a stator with high relation between its diameter and the length. However, it presents a reduced conjugate, and a big set of forces applied to the bearings due to the axial forces exerted on the stator and the rotor. Figure 1 (a) shows an example of this topology. The double-side topology is subdividing into two categories: Axial Flux Internal Rotor (AFIR) and Axial Flux Internal Stator (AFIS). The AFIR category has in its configuration a central rotor and two stators, in the rotor are allocating the permanent magnets or coils, on one side of the disk as the other, and the rotor rotates between two stators. These stators can be connecting in series or parallel. However, it is preferable to use the stators in series due to the fact of producing equal and balanced axial forces.

Figure 1 (b) shows this category. The AFIS category, thus, exhibits a stator in the center and two rotors. In this configuration, the stator disk is locating between the two rotor disks, where the permanent magnets or coils are grouping. The main advantage is the versatility of this category since it can be using in a wide range of applications. However, it has the disadvantage of using a larger magnet volume than the previous topology shown in Figure 1 (c). There is still the multistage mode where the increase of the torque achieved through the engine diameter, furthermore, this topology is limited by the axial force borne by the bearings, mechanical integrity of the junction of the discs with the shaft, and stiffness of the rotor and stator. One solution for high torque machines is the alternating insertion of rotor and stator disks. This configuration is favorable where there is available space in the axial direction, shown in Figure 1 (d). These categories can still be subdivided, depending mainly on the configuration of the winding, rotor with

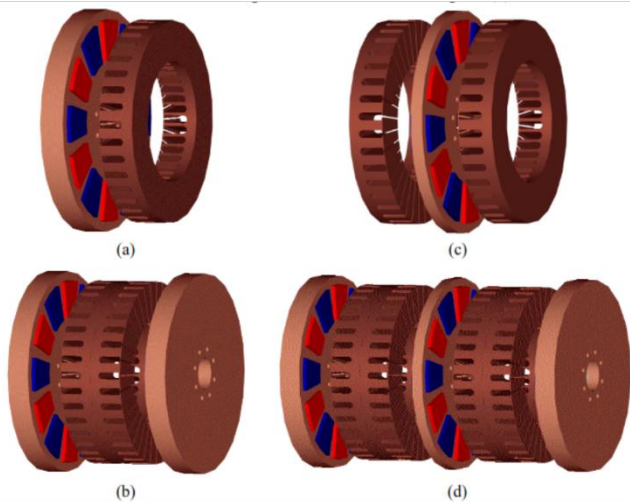grooves or without grooves and presence of ferromagnetic core in the stator or rotor, or both.

Figure 1 – AFSEI Machine Settings. (a) Structure one stator - one rotor; (b) Structure of two rotors - one stator; (c) Structure one rotor - two stators; (d) Multistage structure with multiple rotors and stators [7].

2 MODELING OF A HYDRO-GENERATE SET

Hydraulic turbines are flow converters in rotational mechanical energy. Pelton, Francis, Kaplan, Turgo, Propeller, Michell-Banki, and others are among the several types that can be applying in small, mini, and micro hydroelectric power plants.

In Brazil, the first three are the most used and, for the other types, its use is almost empirical, not involving innovations that make possible the increase of its yield and simplicity of use. Known as a Michell-Ossberger, Michell-Banki or Banki turbine, the cross-flow turbine is qualified as an action turbine for flows in the range of 0.025 to 20 m³/s and falls to water up to 200 m and. Equipment presented by Ossberger Turbinenfabrick and CINK, develops up to 2 MW of power, with yields that can reach up to almost 90 %. Since its invention, the main innovations presented are focusing on the changes in the injector of action water turbine changes, the use of new materials in the blades, the shaft, and the rotor bearings.

2.1 Modeling of the Crossflow Hydrokinetic Converter

In the modeling of a hydrokinetic converter, it is possible to act on two large fronts, the first one relates fluid flow models, and the second is related to the turbine model.

2.1.1 Non-permanent Flow Modeling

The flow conditions in real watercourse systems generally vary with time and space. That flows are called nonuniform and not permanent. These variations may have natural, human, accident or incident origins. Non-permanent flow is complex, and for simplified applications of parameters such as speed and depth are functions of time and distance traveled. The usual mathematical model for the definition of nonpermanent flows is defined by the Saint-Venant equations (ESV), which through dependent variables such as mean velocity and channel depth, and independent variables such as longitudinal distance and time, can express the flows. ESVs are usually presenting on characteristic types; the first type recognizes that there are only the direction variations on the x-axis, these equations are calling ESVs of one dimension, ESV-1D, as shown in equation (1),

$$\begin{cases} \dfrac{\partial h}{\partial t} + \dfrac{\partial}{\partial x}(Uh) = 0 \\ \dfrac{\partial U}{\partial t} + U\dfrac{\partial U}{\partial x} + g\dfrac{\partial h}{\partial x} = g(S_{0x} - S_{fx}) \end{cases} \tag{1}$$

where, h is the channel depth, g is the gravitational constant, U is the velocity in the x-direction. $\partial h / \partial x$ is the slope of the water surface, $\partial h / \partial t$ is the depth variation over time, $\partial U / \partial x$ is the velocity variation over distance, $\partial U / \partial t$ is the velocity variation over time, S_{0x} is the slope of the channel and S_{fx} is the friction slope.

The second type of ESV is understood that fluid can undergo variations between the directions x and y in time. This equation is called ESV of two dimensions or ESV-2D and is given by:

$$\begin{cases} h_t + (Uh)_x + (Vh)_y = 0 \\ \dfrac{\partial U}{\partial t} + U\dfrac{\partial U}{\partial x} + V\dfrac{\partial U}{\partial y} + g\dfrac{\partial h}{\partial x} = g(S_{0x} - S_{fx}) \\ \dfrac{\partial V}{\partial t} + U\dfrac{\partial V}{\partial x} + V\dfrac{\partial V}{\partial y} + g\dfrac{\partial h}{\partial y} = g(S_{0y} - S_{fy}) \end{cases} \tag{2}$$

where, h is the channel depth, g is the gravitational constant, U is the velocity in the x-direction, V is the velocity in the y-direction, $\partial h / \partial x$ is the slope of the water surface in the x-direction, $\partial h / \partial y$ is the slope of the water surface in the y-direction, $\partial h / \partial t$ is the depth variation over time, $\partial U / \partial x$ is the velocity variation over distance in the x-direction, $\partial U / \partial y$ is the velocity variation over distance in the y-direction, $\partial V / \partial x$ is the velocity variation over distance in the x-direction, $\partial V / \partial y$ is the velocity variation over distance in the y-direction, $\partial U / \partial t$ is the velocity variation over time, $\partial V / \partial t$ is the velocity variation over time, S_{0x} is the slope of the

channel in the x-direction, S_{fx} is the friction slope in the x-direction, S_{0y} is the slope of the channel in the y-direction and S_{fy} is the friction slope in the y-direction.

Note that the resolution of this model in its analytical form comes through high order differential equations, which makes its solution very complicated [8].

One of the ways for a feasible ESV solution comes with the use of hypotheses and approximations being the most elegant of them the Navier-Stokes equations of hydrodynamics.

In the Navier-Stokes equations, the hypothesis considered is there is a linear relationship between the fluid stress and the fluid velocity gradient, and that fluid is isotropic. Thus, this shear stress and the velocity gradient can be related to the viscosity and the second viscosity coefficient. This relation is given by [9]:

$$\sigma_{xx} = -p + 2\mu\frac{\partial u}{\partial x} + \lambda\nabla.\nabla \quad \tau_{xy} = \mu\left(\frac{\partial u}{\partial y} + \frac{\partial v}{\partial x}\right) \quad (3)$$

$$\sigma_{yy} = -p + 2\mu\frac{\partial v}{\partial y} + \lambda\nabla.\nabla \quad \tau_{xz} = \mu\left(\frac{\partial u}{\partial z} + \frac{\partial w}{\partial x}\right)$$

$$\sigma_{zz} = -p + 2\mu\frac{\partial w}{\partial z} + \lambda\nabla.\nabla \quad \tau_{yz} = \mu\left(\frac{\partial v}{\partial z} + \frac{\partial w}{\partial y}\right)$$

where σ is the shear stress of the fluid, p is the, μ is the viscosity, u, v and w are the velocities in the directions $x, y,$ and z, respectively, τ_{xy} is the torsion in the direction x and y, τ_{xz} is the torsion in the direction x and z and τ_{yz} is the torsion in the direction y and z. For monatomic gases, the second viscosity coefficient is given by:

$$\lambda = -\frac{2}{3}\mu \qquad (4)$$

as the Stokes hypothesis is given by:

$$-\frac{1}{3}\left(\sigma_{xx} + \sigma_{yy} + \sigma_{zz}\right) = p \qquad (5)$$

because it is a liquid the scalar product, $\nabla.\nabla$ is equal to zero and, in the hypothesis that the fluid is homogeneous, one can define the Navier-Stokes equations, which are given by:

$$p\frac{Du}{Dt} = -\frac{\partial p}{\partial x} + pg_x + \mu\left(\frac{\partial^2 u}{\partial x^2} + \frac{\partial^2 u}{\partial y^2} + \frac{\partial^2 u}{\partial z^2}\right) \qquad (6)$$

$$p\frac{Dv}{Dt} = -\frac{\partial p}{\partial y} + pg_y + \mu\left(\frac{\partial^2 v}{\partial x^2} + \frac{\partial^2 v}{\partial y^2} + \frac{\partial^2 v}{\partial z^2}\right)$$

$$p\frac{Dw}{Dt} = -\frac{\partial p}{\partial z} + pg_z + \mu\left(\frac{\partial^2 w}{\partial x^2} + \frac{\partial^2 w}{\partial y^2} + \frac{\partial^2 w}{\partial z^2}\right)$$

Note that there are three equations for four unknowns (u, v, w, p) and that the terms of the equations are partial derivatives. For the problem of the four unknowns, we must admit two more equations, that of continuity and that of energy.

The continuity equation for incompressible fluids is given by:

$$\frac{\partial u}{\partial x} + \frac{\partial v}{\partial y} + \frac{\partial w}{\partial z} = 0 \qquad (7)$$

The energy equation is expressed by:

$$\rho\frac{D\tilde{u}}{Dt} = K\left(\frac{\partial^2 T}{\partial x^2} + \frac{\partial^2 T}{\partial y^2} + \frac{\partial^2 T}{\partial z^2}\right) \\ - \rho\left(\frac{\partial u}{\partial x} + \frac{\partial v}{\partial y} + \frac{\partial w}{\partial z}\right) \qquad (8)$$

where K is the thermal conductivity, T is the temperature, and $\rho\,dxdydz$ is the mass of the particle of fluid.

The solution of the problems of fluid flow, it is necessary to investigate three equations, the continuity equation, the Navier-Stokes equations, and the energy equation. Due to the nonlinearity of the partial derivatives, a trivial solution cannot be obtained.

The resolution of the Navier-Stokes model for non-permanent flow can be simplified when using computational approximate numerical techniques, known as computational fluid dynamics (CF) tools. The FC presents several methods for solving the partial differential equations, for example, method of the characteristics, finite differences, finite elements, limited volumes, among others. The most used are the finite difference and finite volume methods [9].

2.1.2 Crossflow Hydrokinetic Banki converter

The Banki turbine is an atmospheric radial flow wheel that derives its power from the kinetic energy of the water jets. From the speed point of view, this turbine can be placed between the Pelton tangential water turbine and the Francis mixed flow wheel. The Banki turbine presents unique characteristics because they require small differences between downstream and upstream, and may be of interest to most engineers, especially those in mountain states [10].

The Banki turbine consists of two parts the nozzle of the water jet and the rotor of the turbine. This rotor is forming by two discs interconnected, at its edge, by several curved blades. The fluid is injected at a sixteen-degree angle by tangentiality the water wheel.
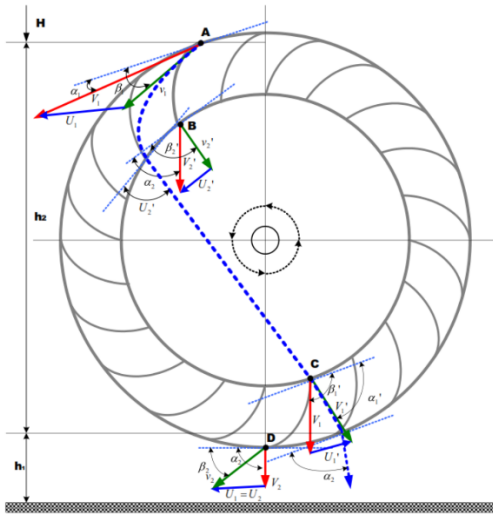
Figure 2 shows the design developed by Banki [10].

Figure 2 - Path of water through the turbine [9, 10].

Assuming that, the input jets in the turbine enter through point A and the angle of incidence is $\propto$, the absolute velocity (V) of the fluid is expressed by:

$$V = C\sqrt{2gH} \tag{9}$$

where C is the coefficient relative to the jet, in the range of 0.98, g is the gravitational constant and H is the height of the jet inlet.

Observing Figure 2, once the peripheral velocity at a point of the wheel is known, it is possible to determine the relative velocity (v_1). On the other hand, the angle of the blades must be equal to β_1.to obtain the maximum efficiency of the turbine. According to Donat Banki [10] the effectiveness of the turbine can be calculated as follows:

By making the inlet angle of the water jet relative to the vanes equal to 16°, we obtain maximum efficiency, with $\cos \alpha_1$ equal to 0.96, $\cos^2 \alpha_1$ equal to 0.98, C is equal to 0.98 and ψ is equal to 0.98, this efficiency reaches 87.8 %. However, studies by [11] show that the most efficient point is 15°.

2.2 Electrical modeling of the axial flux generator

The axial flux generator has a geometric configuration in disks, which has advantages when operated at low speeds compared to radial flow generators. The union of the axial geometry and permanent magnets allows the generator to use the magnets ability to create the magnetic field in the rotor, requiring no electric current circulation as in the case of winding rotors. Then, the magnetic flux travels in a direction perpendicular to the direction of rotation of the rotor.

The axial flux generator presents the windings of the stator phases in a distributed form, obeying an approximately sinusoidal distribution. This constructive characteristic produces a sinusoidal electromotive force like those provided in asynchronous machines and conventional synchronous machines (CSM).

The model per phase of the machine is used to perform mathematical modeling from the theory of CSM [12, 13]. By replacing the rotor windings of a CSM with magnetic elements, the equations for the electric model of the generator has formed.

The total flux in a coil is equal to the sum of the partial fluxes, and it is given to:

$$\emptyset_t = \sum \emptyset_i \tag{11}$$

According to equation (11), taking the phase to flux in the winding of the stator "a" phase is composed of the flux produced by the current circulating in it, the concatenated fluxes of the stator "b" and "c" and the concatenated fluxes produced by the rotor magnets. Thus, the equations for the fluxes of the three-phase generator armature coils are:

$$\begin{cases} \emptyset_a = L_a i_a + M_{ab} i_b + M_{ca} i_c + \emptyset_{pma} \\ \emptyset_b = M_{ab} i_a + L_b i_b + M_{bc} i_c + \emptyset_{pmb} \\ \emptyset_c = M_{ca} i_a + M_{bc} i_b + l_c i_c + \emptyset_{pmc} \end{cases} \tag{12}$$

Writing the equation (2) in matrix form:

$$\begin{bmatrix} \emptyset_a \\ \emptyset_b \\ \emptyset_c \end{bmatrix} = \begin{bmatrix} L_a & M_{ab} & M_{ca} \\ M_{ab} & L_b & M_{bc} \\ M_{ca} & M_{bc} & L_c \end{bmatrix} \begin{bmatrix} i_a \\ i_b \\ i_c \end{bmatrix} + \begin{bmatrix} \emptyset_{pma} \\ \emptyset_{pmb} \\ \emptyset_{pmc} \end{bmatrix} \tag{13}$$

Where,

L_i is the proper inductance of a stator coil;

M_{ij} is the mutual inductance between the two stator coils;

$\emptyset_{pmi}$ is the magnetic flux concatenated by the phases and generated by the rotor.

In the vector form, equation (13):

$$\emptyset_{abc} = L_{abc} i_{abc} + \emptyset_{pm} \tag{14}$$

The own and mutual inductances of the axial flux generator do not depend on the electrical angle θ_e, since

the rotor of the machine is of smooth poles, thus being able to consider:

$$L_a = L_b = L_c = L_L \qquad (15)$$

$$M_{ab} = M_{bc} = M_{ca} = M \qquad (16)$$

The concatenated magnetic fluxes generated by the permanent magnets depend on the electrical angle θ_e, of the machine and are given by:

$$
\begin{cases}
\emptyset_{pma} = \emptyset_{pm}\cos(\theta_e) \\
\emptyset_{pmb} = \emptyset_{pm}\cos\left(\theta_e - \dfrac{2\pi}{3}\right) \\
\emptyset_{pmc} = \emptyset_{pm}\cos\left(\theta_e + \dfrac{2\pi}{3}\right)
\end{cases} \qquad (17)
$$

Where, $\emptyset_{pm}$ is the maximum magnetic flux generated by the rotor magnets.

Figure 3 represents the equivalent electrical circuit of a permanent magnet synchronous machine.
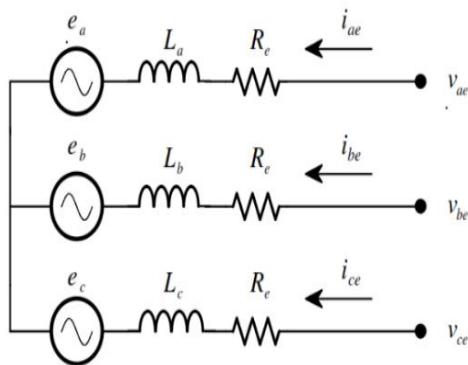
Figure 3 - Electrical model of synchronous three-phase permanent magnet machine.

where e_a, e_b and e_c are the voltages resulting from the variation of the concatenated flux generated by the rotor magnets and R_e denote the stator winding resistance.

With the electric model of the permanent magnet synchronous machine shown in Figure 3, the following equations for the stator voltages are obtained as follows:

$$
\begin{cases}
v_a = R_e i_{ae} + \dfrac{d\emptyset_a}{dt} \\
v_b = R_e i_{be} + \dfrac{d\emptyset_b}{dt} \\
v_c = R_e i_{ce} + \dfrac{d\emptyset_c}{dt}
\end{cases} \qquad (18)
$$

Writing the equation (18) in matrix form:

$$
\begin{bmatrix} v_a \\ v_b \\ v_c \end{bmatrix} =
\begin{bmatrix} R_e & 0 & 0 \\ 0 & R_e & 0 \\ 0 & 0 & R_e \end{bmatrix}
\begin{bmatrix} i_{ae} \\ i_{be} \\ i_{ce} \end{bmatrix} +
\frac{d}{dt}
\begin{bmatrix} \emptyset_a \\ \emptyset_b \\ \emptyset_c \end{bmatrix} \qquad (19)
$$

The generalization of equation (19) is given by:

$$v_{abc} = R i_{abc} + \frac{d}{dt}\emptyset_{pm} \qquad (20)$$

Equations (13) and (19) form a three-phase model representing the permanent magnet synchronous generator.

The model presented in coordinates *abc* has the inductances dependent on the electric angle θ_e. A biphasic model of the machine can be obtained from the three-phase, making the inductances fixed with time, to facilitate the analysis of the machine.

By applying the Park transformations to a three-phase vector model, two coordinate axes are rotated with a given angular velocity. The reference plane formed by the rotating axes is aligned with the rotor's magnetic axes and rotates with an electric angular velocity of ω_e. The direct axis d is kept in phase with the flux of the magnetic field generated by the rotor, and the quadrature axis q is kept in phase with the flux of the magnetic field generated by the rotor. The flux in the direct axis of coordinates *dq* is equal to the maximum flux generated by the rotor since in the quadrature axis it is null.

Figure 4 shows the relationship between the synchronous coordinate plane *dq* and the coordinate plane *abc*.
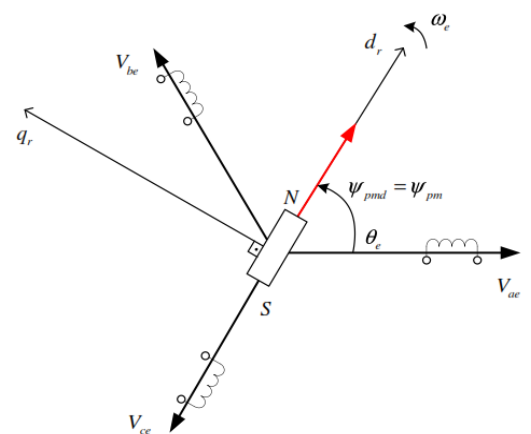
Figure 4 - The relationship between the synchronous coordinate plane dq and the coordinate plane abc [13].

The direct application of Park in equations (13) and (19) is defined by:

$$[T_{abc \to dq}]\psi_{abc} = [T_{abc \to dq}](L_{abc} i_{abc}) \tag{21}$$
$$+ [T_{abc \to dq}]\emptyset_{pm}$$

$$[T_{abc \to dq}]v_{abc} = [T_{abc \to dq}](R i_{abc}) \tag{22}$$
$$+ [T_{abc \to dq}]\frac{d}{dt}\emptyset_{abc}$$

Simplifying equations (21) and (22) of coordinate changes, one can obtain:

$$\begin{bmatrix} \emptyset_{de} \\ \emptyset_{qe} \end{bmatrix} = \begin{bmatrix} L_d & 0 \\ 0 & L_q \end{bmatrix} \begin{bmatrix} i_{de} \\ i_{qe} \end{bmatrix} + \begin{bmatrix} \emptyset_{pm} \\ 0 \end{bmatrix} \tag{23}$$
, and

$$\begin{bmatrix} v_{de} \\ v_{qe} \end{bmatrix} = R_e \begin{bmatrix} i_{de} \\ i_{qe} \end{bmatrix} + \omega_e \begin{bmatrix} 0 & 1 \\ -1 & 0 \end{bmatrix} \begin{bmatrix} \emptyset_{de} \\ \emptyset_{qe} \end{bmatrix} + \frac{d}{dt} \begin{bmatrix} \emptyset_{de} \\ \emptyset_{qe} \end{bmatrix} \tag{24}$$

Substituting (23) into (24) gives the model in coordinates dq of the generator:

$$\begin{cases} v_{de} = R_e i_{de} + L_d \dfrac{di_{de}}{dt} - \omega_e L_q i_{qe} \\ v_{qe} = R_e i_{qe} + L_q \dfrac{di_{qe}}{dt} - \omega_e(L_d i_{de} + \emptyset_{pm}) \end{cases} \tag{25}$$

where one can obtain,

$$\begin{cases} L_d = \dfrac{3}{2}(L_0 - L_m) \\ L_q = \dfrac{3}{2}(L_0 - L_m) \end{cases} \tag{26}$$

Given the equation of the model, it is possible to verify a difference between the permeability of the magnetic axes dq due to the variation of temperature and that there is no variation of the mutual inductance with the movement of the rotor thus, the magnetic inductances L_d and L_q are equals practically and can be expressed by:

$$L_m = 0 \quad e \quad L_d = L_q = L_{eq} \tag{27}$$

From the system of equations (25) one can obtain the electric model in coordinates dq. Figure 5 shows the equivalent electrical circuit.
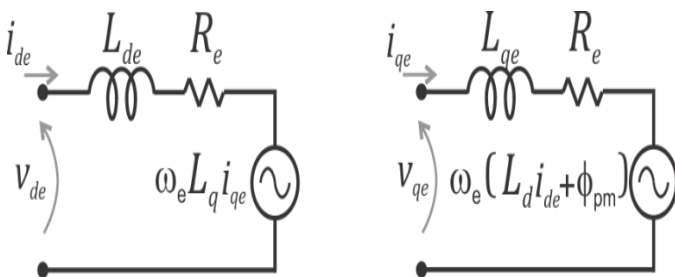

Figure 5 - The electrical model of the axial flux generator in coordinates dq [13].

The sum of the products between the instantaneous voltage and the instantaneous current of each phase is the power of the axial flux generator.

$$P_e = v_{ae} i_{ae} + v_{be} i_{be} + v_{ce} i_{ce} \tag{28}$$

The matrix expression derived from (28) is defined by:

$$P_e = [v_{ae} + v_{be} + v_{ce}] \begin{bmatrix} i_{ae} \\ i_{be} \\ i_{ce} \end{bmatrix} \tag{29}$$

The electric power of the generator in synchronous coordinates dq is:

$$P_e = i_{de} \frac{d}{dt}\emptyset_{de} + i_{qe} \frac{d}{dt}\emptyset_{qe} \tag{30}$$

The electric power is obtained by the manipulation of equations (25) and (30) and is expressed by:

$$P_e = \frac{3}{2}\Big[R_e(i_{de}^2 + i_{qe}^2) \tag{31}$$
$$+ \Big(i_{de}\frac{d}{dt}\emptyset_{de} + i_{qe}\frac{d}{dt}\emptyset_{qe} \Big)$$
$$+ \omega_e(\emptyset_{de} i_{qe} - \emptyset_{qe} i_{de}) \Big]$$

Equation (31) can be separated in terms of power dissipated by stator resistance or losses in P_{CU} copper, as follows:

$$P_{CU} = \frac{3}{2} R_e(i_{de}^2 + i_{qe}^2) \tag{32}$$

P_i expresses the rate of change of the energy stored in the inductances of the generator and given by:

$$P_i = i_{de}\frac{d}{dt}\emptyset_{de} + i_{qe}\frac{d}{dt}\emptyset_{qe} \tag{33}$$

The electromechanical power of the generator (P_g) is calculated by:

$$P_g = \frac{3}{2}\omega_e(\emptyset_{de} i_{qe} - \emptyset_{qe} i_{de}) \tag{34}$$

The electric conjugate is given in two components (12). The first is called the magnetic field excitation conjugate and is calculated by:

$$T_{e1} = \frac{3}{2}\frac{N_p}{2}(\emptyset \ i_{qe}) \tag{35}$$

The reluctance conjugate is the second component, expressed by:

$$T_{e2} = \frac{3}{2}\frac{Np}{2}(L_d - L_q)i_{de}i_{qe} \qquad (36)$$

therefore,

$$T_e = \frac{3}{4}Np(\emptyset\ i_{qe}) + (L_d - L_q)i_{de}i_{qe} \qquad (37)$$

where Np is the number of poles of the AFSEI.

For the case of the permanent magnet synchronous machine with a rotor of smooth poles, the conjugate of reluctance is null.

2.3 Modeling of the axial flux self-excited induction generator

The apparent power developed in an AFSEI, given in (kVA), is expressed about its inner and outer diameters as follow:

$$P_a = 2\ m\ E_p\ I_p * 10^{-3} \qquad (38)$$

where m is the number of phases, E_p is the phase electromagnetic force (V), and I_p is a phase current (A).

The phase electromagnetic force (V)

$$V_p = E_p = 4.44\ k\ \frac{N_{p*n}}{2}\ \emptyset\ N \qquad (39)$$

where k is the winding factor, N_p is the number of poles, n is the speed (rps), $\emptyset$ is the flux per pole (Wb), and N is the number of turns per phase.

Other definitions are necessary, for example, specific magnetic loading and specific electric loading. The specific magnetic loading is defined as the total flux per unit area over the surface of the armature periphery and known as average flux density as follows:

$$B = \frac{N_p\ \emptyset}{\frac{\pi}{4}(D_{out}^2 - D_{in}^2)} \qquad (40)$$

where B is given (Wb/m^2).
The definition of specific electric loading is the number of armature conductors per meter of armature periphery at the air gap. Specific electric loading is equal the total number conductors of current divided the armature periphery at air gap as follows:

$$A = \frac{2\ m\ N_p\ I_p}{\frac{\pi}{2}(D_{out} + D_{in})} \qquad (41)$$

where A is given (A/m).

On substitution in the equations (39), (40), and (41) in (38) is given:

$$P_a = k_a\left(D_{out} + D_{in}\right)^2\left(D_{out} - D_{in}\right)n \qquad (42)$$

where:

$$k_a = 2.74\ k\ B\ A * 10^{-3} \qquad (43)$$

In the other hand, the most important parameters in the design of an AFSEI is the diameter ratio and is given:

$$k = \frac{D_{out}}{D_{in}} \qquad (44)$$

In [14], the diameter ratio recommended for small machines is 1.4 to 1.7 and 1.7 to 2.0 for medium and large machines.

Rewritten the equation (42) in term of diameter ratio (k) as:

$$P_a = \frac{k_a(k^2 - 1)(k + 1)}{k^3}n\ D_{out}^3 \qquad (45)$$

3. PROJECT AND VALIDATION OF THE HYDRO-GENERATOR

The developed generator model deals with a floating electric power generation system, containing an axial flow electric generator coupled to an axial flow hydrokinetic converter, capable of generating electrical energy from the use of even reduced water flows. Figure 6 shows the hydro-generator assembly.
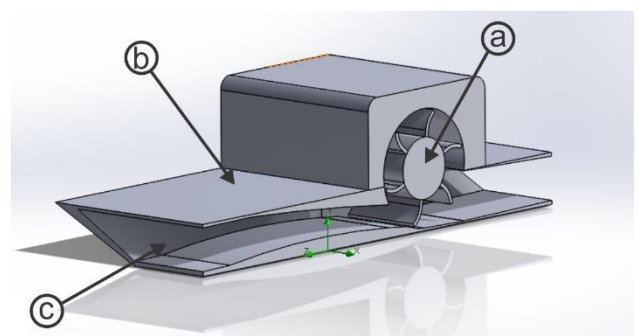

Figure 6 - Model of the hydrokinetic converter. a) AFPM generator conjugated to the axial flow turbine; b) Hydro-generator assembly floating box; c) Flow inlet.

The floating electric power generation system consists of three parts:

1) Floating box, whose function, besides supporting the turbine generator, is to multiply the speed of the water flow, in an amount equal or superior to four times.

2) Turbine electricity generation, consisting of the axial electric generator constructed from the center of rotation of a turbine.

3) Voltage and frequency converter.

The architecture of the Floating Box has an opening in its front part and a tunnel that directs the flow to a window with a system of horizontal wings, inferior and superior, that satisfy the formation of lamellar jets in part superior and inferior of an access window to the blades of the generating turbine.

In the hydrokinetic converter simulation shown by Figure 7, one can see the wing shape formed by the float region. Figure 7 is shown in Figure 8, where it is noted that in the simulation process the velocity of the water flow is 2 m / s, emphasized by two points located on the surface of the hydro converter inlet.
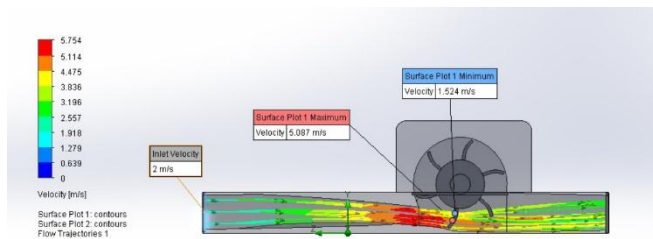

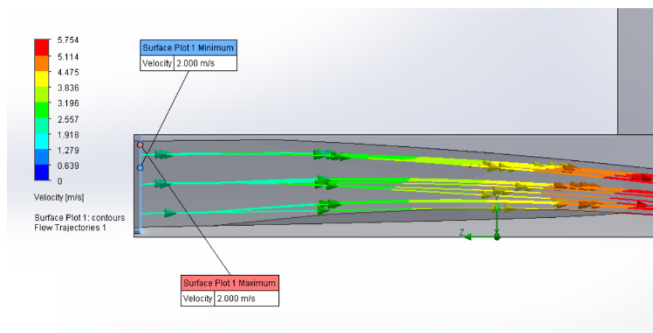Figure 7 - Simulation of the hydrokinetic converter.

Figure 8 - Detail of the hydrokinetic converter input with an initial velocity of 2 m/s.

In Figure 9 it may be noted that the flow velocity reaching one of the blades of the axial flow generating turbine is 32 m/s, which implies 16 times the initial speed with a laminar flow which is desirable. The results of the simulations, using the mathematical models embedded in the simulation software, showed that the alternative chosen for the case of the hydrokinetic converter meets the need for increased flow velocity, which will consequently increase the generator rotor rotation and more flexibility in the sizing step of the electric machine.
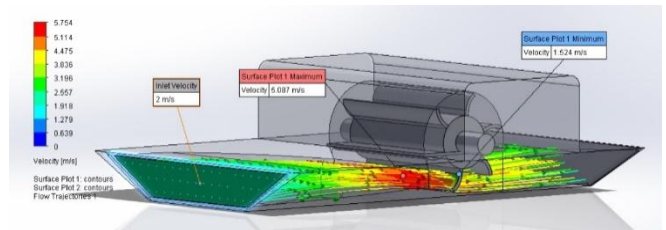

Figure 9 - Detail of two points near the leading edge of one of the blades of the axial flux turbine.

The electrical AFPM generator is built on the same rotor axis as a cross-flow turbine, its consisting of an authentic water wheel, dispensing the use of belts, chains, gears or axles for connection to the generator.
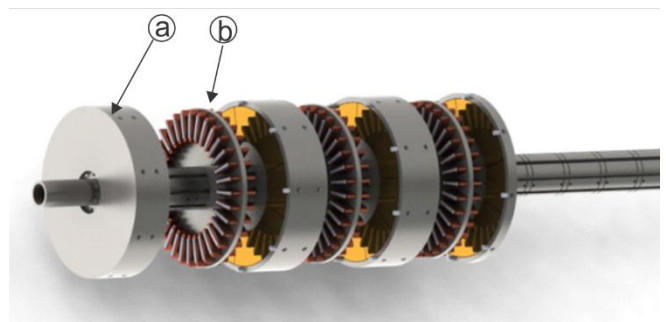

Figure 10 - The core of the AFPM generator. a) rotor and b) stator.

The hydrokinetic converter is composed of Power Units coupled to the blades, forming the electric machine, which consists of:

1) a disc with a central hole with cutters for engaging a fixed axis, containing housing for the conductor coils.

2) a central bearing disc for fixed shaft engagement, containing housing for permanent magnets.

The design of the rotor will have the drive with a rotation (N_s) of 103.34 up to 450 rpm, in this way, it was established a high number of poles (p) equal to 16, obtaining an electric frequency of 60 Hz, and being calculated through the equations shown in items 2.2 and 2.3.

Table 1 shows the characteristics considered for the project, and it can be noted that it is a three-phase generator and that has the objective of proof of concept of hydro-converter.

Table 1 - Constructive characteristics of the project.

parameters	Value	Unit	Descriptions
Ns	16	Polos	Number of poles
p	8	Ppar	Number of pole pair

nreels	9	bob	Number of reels
m1	3	fase	Number of electrical phases
Dout	0.2280	m	External diameter
Din	0.1680	m	Internal diameter
Inom	3.0000	A	Nominal Current
Bmg	1.4500	T	Flux Density Peak magnetic N52
α_i	0.8500	%	Factor between maximum and average flux density
Ka	0.2000	%	Factor of the Electric machine
kw	0.8500	%	Kw – Winding factor. For most three-phase machines factor varies from 0.85 to 0.95
N	70	turns	Number of turns
Kdisp	0.9000	%	Dispersion factor of magnetic flux 0.80 ↔ 0.95
kpm	0.9000	%	Dispersion Factor
g air gap	0.0020	m	air gap
Wcu	0.0700	m	Dimension of coil head
Rbob	0.6	Ω	Rotor winding resistance
Lbob	0.142	mH	Stator coil inductance

With the sizing and an increase of the magnetic package, the calculated characteristics can be seen in Table 2 - Calculation of the constructive parameters of the power units of the hydro-generator.

Table 2 - Calculation of the constructive parameters of the power units of the hydro-generator.

Parameters	Value	Unit	Description
Nf	3		Number of reels per phase stage
Am	122.77	A/m	Density of Linear current
fif1	0.0049	Wb	Magnetic Flux
Ap	0.0039	m2	Polar Area
Ea	0.0474	V	Generated voltage or back electromotive force
wm	48.7972	Rad/s	Angular speed
Ef	3.4157	V	Induced voltage
Kd	0.7368	%	Factor between the diameters
Bu	6.9617	T	Density of magnet magnetic flux

Pnom	30.7416	W	Power per Unit
Ptot	245.933	W	Power of the set

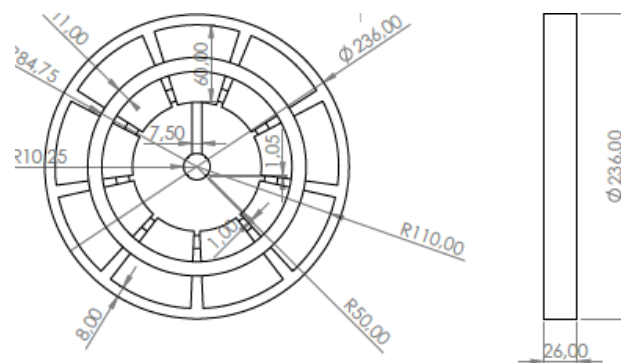Figure 11 and Figure 12 show the stator and rotor constructional design details.
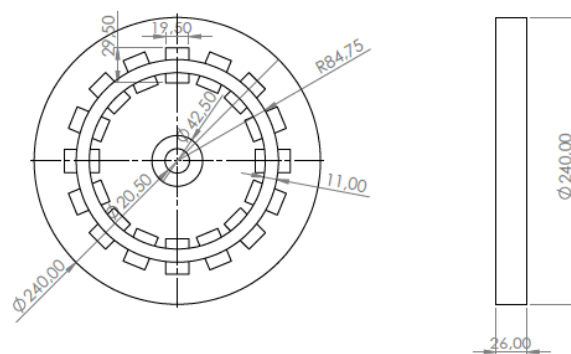

Figure 11 - Stator Coil Disc.

Figure 12 - Housing plate of magnets of the electrical machine -rotor.

Figure 13 - shows the constructive detail of both the rotor and the stator where it is noted that there are protruding poles for increasing the desired power. It should be remembered that the structure of the disc is cast in ABS, for testing purposes, and a new concept of lighter turbines.

Figure 13 - Detail of the power unit.

The proposed generator has eight power units called u.p. containing one stator and one rotor forming a stage. The magnetic flux path for the first rotor is closed by the way between the first rotor, air gap, first stator, air gap, and first rotor. The central rotor is characterized by the magnetic flux that crosses its structure only axially, having its closed flow path by the central rotor, gap, a second stator, gap, central rotor, gap, first stator, gap, and central rotor.

Power units nested on the same axis form the turbine rotor core. To these units, a set of blades are coupled, forming the hydrokinetic converter, by the rotation of the magnet discs, or induction system, with bearings.

In the bench test of the AFPM generator, shown in Figure 14, a 1 Ω three-phase load with a power of 30W was used during the trial; the angular velocity was increased to the maximum electrical power that the load could withstand. At reaching this value, the angular velocity, phase voltage and phase current measurements were recorded, as shown in Figure 15 , Figure 16, and Figure 18. It is noted that the velocity at the angular velocity reached corresponds to approximately 25% of the expected and that its value is 110.37 rpm, producing a three-phase power of 34.47 W. Thus, extrapolating to the set, under these conditions, a total electrical power of 275.79 W per power unit can be obtained.

Figure 14 - Controlled bench test of the AFPM Generator.

Figure 15 - Tachometer indicating the angular velocity of 110.37 rpm used in the test.

Figure 16 - RMS voltage generated by one of the phases of the hydro-generator.

Figure 18 - Generator phase current.

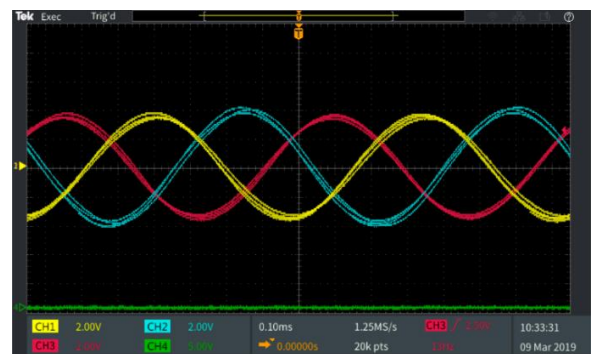Figure 17 shows the sinusoidal behavior of the generated voltage.

Figure 17 - The three-phase voltage generated in loads of 1 Ω of 30 W.

Figure 18 and Figure 19 show the test environment of models of the hydro-generators.

Figure 18 - Hydraulic test bench.

Figure 19 - Test of the AFPM generator in the hydraulic bench.

Solutions that offer new sustainable forms of energy generation must always be evaluated with considerable discretion, especially from its application. The system was initially tested in a controlled flow channel in a laboratory, and later in sections of rivers with reduced flow, industrial water flow channels and river stretches downstream of hydroelectric plants, where its efficiency, ease of installation, maintenance routines and the possibility of production in series, aiming at a future insertion in the market, were evaluated.

4. CONCLUSIONS

The applicability of the hydrokinetic generator involves companies in the electric sector, in addition to other industry segments and until it is used as technology applied to distributed generation, being able to generate energy to meet demands, for example, power generation for auxiliary services of companies, or even communities. The installation of several large units, in series and at various points of water flow, can provide compatible electrical energy to large hydroelectric projects.

Due to its versatility, it is possible to use it in any economic activity that has natural channels or waterways with low flow velocity. A relevant point is the low cost of manufacturing and installation, there is no need for dams, in addition to the low environmental impact. This solution provides the generation of energy in small and medium scale, and hydrokinetic conversion can be applied in tides, ocean currents, small rivers, channels, among others.

REFERENCES

[1] BRASIL JUNIOR, A. et al. **Turbina Hidrocinética Geração 3**. In: IV Congresso de Inovação Tecnológica em Energia Elétrica. 2007

[2] DOS SANTOS, S. M.; ALMEIDA, J. A.; ANDRADE, D. A.; DIAS L. F. **TURBINA HIDROCINÉTICA AXIA.** Proceedings of the 10o Brazilian Congress of Thermal Sciences and Engineering – ENCIT 2004. Braz. Soc. of Mechanical Sciences and Engineering - ABCM, Rio de Janeiro, Brazil, Nov. 29 - Dec. 03, 2004.

[3] VERMAAK, H. J.; KUSAKANA, K.; KOKO, S. P. **Status of micro-hydrokinetic river technology in rural applications: A review of literature.** Renewable and Sustainable Energy Reviews, v. 29, p. 625-633, 2014.

[4] SMART HYDRO POWER GMBH (LTD.), **Smart Monofloat**, Feldafing, Germany, 2014. https://www.smart-hydro.de/

[5] SORNES, K., **Small-scale Water Current Turbines for River Applications.** ZERO – Zero Emission Resource Organization, Oslo, 2010, January. https://zero.no

[6] P&D TERMO NORTE ENERGIA/ANEEL, Código PD-0563-0214/2014 Patente BR 10 2016 013135 9, em 08/06/2016, aguardando conclusão.

[7] PARVIAINEN, A. **Design of axial-flux permanent-magnet low-speed machines and performance comparison between radial-flux and axial-flux machines.** Thesis, 2005.

[8] LOBEIRO, A. M. **Solução das Equações de SAINT VENANT em um e duas Dimensões Usando o Método das Características.** Tese de Doutorado, Universidade Federal do Paraná – UFPR, Curitiba – PR, 2012.

[9] POTTER, M.C.; WIGGERT, D. C. **Mechanics of fluids**, 3rd ed. Brooks/Cole, USA. 2002.

[10] MOCKMORE, C. A.; MERRYFLIED, F. **The Banki Water Turbine.** BULLETIN SERIES. Oregon State College, n25, p1-16, 1949.

[11] JASA L. *et al.* **Investigate Curvature Angle of the Blade of Banki's Water Turbine Model for Improving Efficiency by Means Particle Swarm Optimization** INTERNATIONAL JOURNAL of RENEWABLE ENERGY RESEARCH, Vol.7, No.1, 2017.

[12] BOLDEA, I.; NASAR, S. A. **Unified treatment of core losses and saturation in the orthogonal-axis model of electric machines.** IEE Proceedings B Electric Power Applications, 134(6), 355-363, November 1987.

[13] BERNARDES, T. A., **Análise e Controle de Gerador Síncrono a Imã Permanente Aplicado a Sistema de Conversão de Energia Eólica,** Dissertação de mestrado em engenharia elétrica, Universidade Federal de Santa Maria – UFSM, Santa Maria – RS, 2009.

[14] C. C. Chan, **"Axial-Field Electrical Machines - Design and Applications,"** in IEEE Transactions on Energy Conversion, vol. EC-2, no. 2, pp. 294-300, June 1987. doi: 10.1109/TEC.1987.4765844.

[15] AYDIN, M.; HUANG, S.; LIPO, T. A., **Design and 3d electromagnetic field analysis of non-slotted and slotted torus type axial flux surface mounted permanent magnet disc machines.** *International Electrical Machine and Drive Conference Proceedings*, pages 645–651, 2001.

[16] AYDIN, M. **Axial Flux Surface Mounted Permanent Magnet Disc Motors for Smooth Torque Traction Drive Applications.** Ph.D. thesis, UNIVERSITY OF WISCONSIN, 2004.

[17] GIERAS, J. F.; WANG, R. J.; KAMPER, M. J. **Axial Flux Permanent Magnet Brushless Machines.** Springer, 2008.

[18] CHALMERS, B. J. and SPOONER, E., **"An axial-flux permanent-magnet generator for a gearless wind energy system,"** in IEEE Transactions on Energy Conversion, vol. 14, no. 2, pp. 251-257, June 1999.

[19] KARIM, A.; AZZOUZI, J.; BARAKAT, G. and DAKYO, B., **"Complete Analytical Modeling of an Axial Flux PM Synchronous Machine for Wind Energy Application,"** 2006 12th International Power Electronics and Motion Control Conference, Portoroz, 2006, pp. 996-1001.

[20] LEONARDI, F. and LIPO, T. A., **A comparison of power density for axial flux machines based on general purpose sizing equations.** *IEEE Transactions on Energy Conversion*, 14(2):185–192, 1999.

[21] BIM, E., **Máquinas Elétricas e Acionamento.** Rio de Janeiro, Elsevier, pages 139-144, 2009

BIOGRAPHIES

Dr. Antonio Carlos Duarte Ricciotti is an electrical engineer (1988 - FEI), M.Sc. of (2006) in biomedical and automatic engineering Ph.D. (2017) in power electronics by the Federal University of Santa Maria (UFSM).


Eng. Herbert Militão is an electrical Engineer from the Federal University of Santa Catarina, with over 10 years of experience in commissioning power generating units. He worked in the commissioning of Jirau HPP, Pampa Sul TPP among others in Brazil and South America. He is currently a researcher at GPTI-UNIR

M.Sc. Viviane Barrozo S. D. Ricciotti is an electrical engineer (2008-UFRGS), B.Sc. in Physics (1997-UFPR), B.Sc. in Mathematics (1995-Paranaense University), M.Sc. in Physics (2001-UFRGS).

Engr. Gerson Pereira de Andrade is an Automation & Control Engineer (2013 UBM), and Process Optimization Coordinator at TERNIUM Brasil.
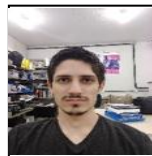
Adailton Braga Júnior was born in Porto Velho, Brazil, on March 4, 1996. He received the B.S. degree in electrical engineering from Federal University of Rondônia, Brazil, in 2019. He is currently a researcher at Control And Automation Laboratory where his work focuses mainly on analysis of disturbances in electric power systems. His research interests include power electronics and signal processing in electric power systems."